Formation and Characterization of Two-Dimensional Arrays of Silver Oxide Nanoparticles under Langmuir Monolayers of n-Hexadecyl Dihydrogen Phosphate

Fei Xiao, Hong-Guo Liu,* and Yong-Ill Lee†

Key Laboratory for Colloid & Interface Chemistry of Education Ministry, Shandong University, Jinan 250100, China
**E-mail: hgliu@sdu.edu.cn*
†Department of Chemistry, Changwon National University, Changwon 641-773, Korea
Received August 11, 2008

Two-dimensional arrays of silver oxide nanoparticles were prepared by oxidation of silver nanoparticle arrays in air. The silver nanoparticle arrays were formed by illuminating the composite Langmuir monolayers of *n*-hexadecyl dihydrogen phosphate (*n*-HDP)/ethyl stearate (ES)/Ag^{+} at the air-water interface by daylight. The average diameters of the nanoclusters is found to be 2.32 ± 0.89, 2.97 ± 0.78, and 4.94 ± 0.57 nm, respectively, depending on the experimental conditions. X-ray photoelectron spectroscopy (XPS), UV-vis spectroscopy and high-resolution transmission electron microscopy (HRTEM) investigations indicate the formation of silver oxide nanoparticles. The possible formation mechanism of the 2D arrays should be attributed to the templating effect of parallel aligned linear supramolecular rows of n-HDP formed at the air-water interface.

Key Words : Silver oxide nanoparticles, Langmuir monolayer, Air-water interface, 2D arrays

Introduction

Two-dimensional (2D) arrays of metal and semiconductor nanoparticles are of great importance due to their unique properties and applications in nanodevices.[1] For example, 2D organized arrays of magnetic nanoparticles show a high magnetic anisotropy and a high magnetic blocking temperature, which have potential applications in high density memory devices[2] and magnetic recording devices.[3] 2D arrays of silver or other metal nanoparticles show unique electronic properties, which can be used in the future in electronic devices.[4,5] In addition, 2D arrays of gold nanoparticles[6] and 2D photonic crystal superlattice[7] exhibit non-uniform enhancement in Raman scatting with spatial distribution of the localized electric field or negative refraction properties, which have potential applications as surface enhanced Raman scattering substrate and optical devices. Several methods have been used to fabricate these arrays in solution and at the interfaces, including template (soft and hard templates) and template-free methods.[8] The most common strategy is to spread surfactant-modified uniform nanoparticles dispersed in organic solvents onto solid substrates[9-11] or air/water interface.[12,13] Perfect 2D ordered arrays formed after evaporating the solvents due to the self-assembly of the nanoparticles. In addition, some unique methods have been developed to prepare 2D arrays of inorganic nanoparticles, such as decomposition of Ag strips at higher temperature,[14] and plasma treatment of 2D arrays of composite surface micelles of block copolymer/metal ions deposited on solid substrates.[15] On the other hand, to develop more convenient method to prepare 2D arrays of inorganic nanoparticles has attracted much attention recently. For example, the preparation and assembly of Ag nanoparticles into 2D arrays were completed in a one step process at the liquid-liquid interface[16] or the air-water interface[17] with the help of surfactants; the organometallic compounds at the air-water interface decomposed, resulting in the formation of ordered metal nanoparticles;[18] and parallel aligned 1D chains of semiconductor nanoparticles were prepared at the air-water interface by using a monolayer of a linear polymer formed *in situ* as a template.[19]

Silver nanoparticles show unique optical, electronic and catalytic properties and can be synthesized easily under ambient conditions. Recently, nanoparticles and nanofilms of silver oxide have attracted much attention due to their unique optical properties, such as abnormal third-order nonlinearity[20,21] and luminescence.[22] Especially the composite silver/silver oxide nanosystems show photoactivated multicolored dynamic fluorescence, which can be applied as a new type of optical data storage materials.[23-25] It was demonstrated that the transformation between silver and silver oxide occurs when exposing to air and illuminating by light.[23]

In our previous studies, 1D chains of silver oxide nanoparticles were prepared by treating the transferred Langmuir-Blodgett monolayers of *n*-HDP/ES/Ag^{+} on solid substrates,[26] and parallel aligned nanowires composed of *n*-HDP/ES/europium complex were obtained at the air-water interface.[27] We demonstrated that *n*-HDP molecules formed parallel aligned linear supramolecules through intermolecular hydrogen bonds, which acted as templates. We think that this kind of supramolecules is a candidate for templates to synthesize and fabricate nanoparticles into ordered arrays under appropriate conditions because the supramolecular structures limit the nucleation and growth regions of the nanoparticles. In this paper, Ag^{+} ions were reduced by daylight irradiation at the air-water interface firstly under Langmuir monolayers of *n*-HDP/ES, and then 2D arrays of silver oxide nanoparticles were obtained by exposing the transferred monolayers in air.

Experimental Section

Chemicals. *n*-hexadecyl dihydrogen phosphate (*n*-HDP) was synthesized according to literature method.[22] Ethyl stearate (ES) was purchased from Aldrich. $AgNO_3$ (99.9%) was purchased from Shanghai Reagent Co. The water used is highly purified with the resistivity ≥ 18.0 MΩ cm. All chemicals were used as received without further purification.

Formation of 2D arrays of silver oxide nanoparticles. π-A isotherms of *n*-HDP/ES monolayers at the air-water and air-$AgNO_3$ aqueous solution interfaces were recorded by using a NIMA 611 Langmuir trough. The beakers filled with $AgNO_3$ aqueous solution with the concentrations of 1×10^{-3} and 1×10^{-4} mol L^{-1} were placed in a clean transparent, sealed container. Then the chloroform solution of *n*-HDP/ES (molar ratio: 1/2) was spreading onto the aqueous solution surface. After evaporation of the solvent, condensed monolayers were formed. The surface pressure was controlled to be *ca.* 10 mN m^{-1} based on the amount of the spreading solution according to the π-A isotherms. The condensed monolayers were illuminated by daylight to get the 2D arrays. Then the films at the air-water interface were transferred onto solid substrates and placed in a dark place in air.

Characterization. The nanostructures transferred on 230-mesh copper grids were characterized by transmission electron microscopy (TEM, JEM-100CXII) with the accelerating voltage of 100 kV, and high-resolution transmission electron microscopy (HRTEM, GEOL-2010) with the accelerating voltage of 200 kV. The nanostructures transferred on quartz slides were characterized by UV-vis spectroscopy (HP8453E) and X-ray photoelectron spectroscopy (XPS, ESCALAB MKII) with Mg Kα ($h\nu$ = 1253.6 eV) as the exciting source at a pressure of 1.0×10^{-6} Pa and a resolution of 1.00 eV.

Results and Discussion

Monolayer behavior of *n*-HDP. The monolayer behavior of n-HDP was studied and the π-A isotherms was given in our previous paper.[26] It was reported that *n*-HDP cannot form stable Langmuir monolayer by itself because of dissolution in water,[26-28] so ES was introduced to prohibit *n*-HDP from dissolution due to the strong interaction between the alkyl chains. The mean molecular area of the composite system of *n*-HDP/ES (1/2) at the air-$AgNO_3$ aqueous solution interface is smaller than that at the pure water surface, indicating the interaction between *n*-HDP molecules and Ag^+ ions and the formation of the composite *n*-HDP/ES/Ag^+ monolayers.

TEM and HRTEM images. Figure 1 shows the TEM micrographs of silver nanostructures formed in the composite Langmuir monolayers at the air-$AgNO_3$ aqueous solution interfaces under daylight illumination. It can be seen that 2D arrays of inorganic nanoparticles formed and the size of the particles changed with experimental conditions. With the Ag^+ concentration of 1×10^{-3} mol L^{-1}, 2D

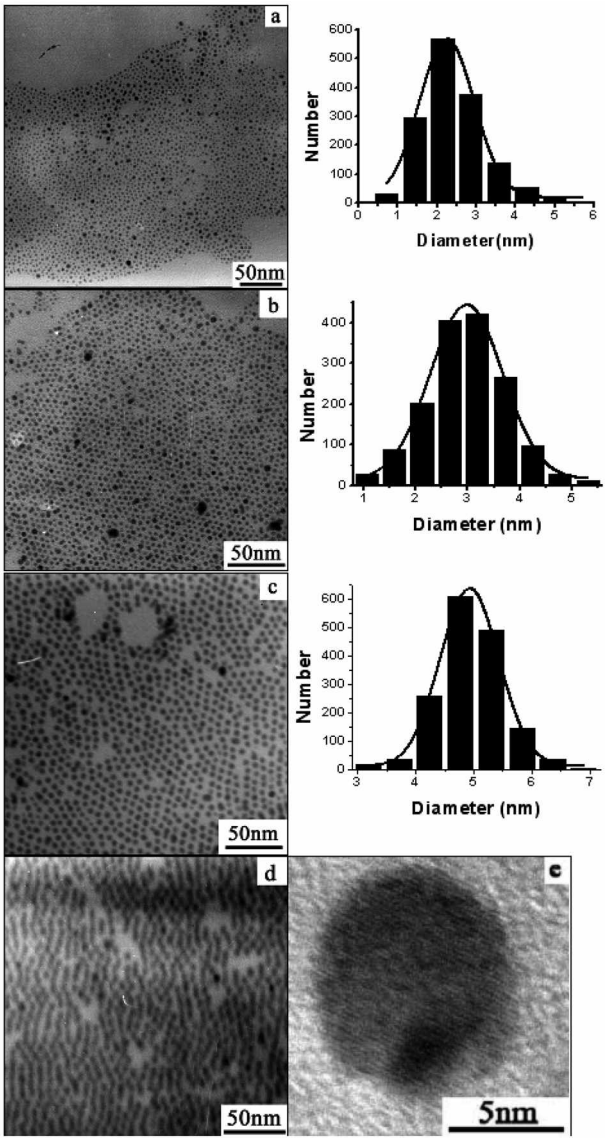

Figure 1. TEM (a-d) and HRTEM (e) micrographs of 2D arrays of nanoparticles transferred from the air-$AgNO_3$ aqueous solution interface after illumination by daylight under the *n*-HDP/ES (1/2) Langmuir monolayers and exposing to air. The subphase concentration: 1×10^{-3} mol·L^{-1} (a, b) and 1×10^{-4} mol·L^{-1} (c-e). Irradiation time: 9 days (a), 31 days (b-e). The size distribution histograms correspond to panels a, b, and c, respectively.

arrays of nanoparticles with the diameter of 2.32 ± 0.89 and 2.97 ± 0.78 nm were formed after illuminating 9 and 31 days, respectively, as shown in Figure 1a and 1b. When the subphase with the concentration of 1×10^{-4} mol L^{-1} was used, nearly mono-dispersive nanoparticles with the diameter of 4.94 ± 0.57 nm were formed, and a quasi-hexagonal pattern appeared after 31 days (Fig. 1c). In addition, flexural linear structure with the width of ~4.5 nm and the length of several tens of nanometers can be seen clearly from Figure 1d, which should be attributed to the attachment of the nanoparticles under the direction of the templates.

It can be seen that the nanoparticles are round ones from the TEM micrographs. We cannot give exact shape of the nanoparticles just based on TEM investigations at present.

However, we can deduce the possible shape of the nanoparticles according to the special growth process of the particles and related literatures. Fendler *et al.* have investigated the shape of ZnS and CdS nanoparticles formed at the air-water interface by using atomic force microscopy (AFM) and the other techniques.[29,30] They found that the nanoparticles are disk-like ones, the thickness of the particles are less than the diameters. This should be attributed to the special growth environments of the particles, because the growth of the nanoparticles was limited at the interface and to the subphase under the Langmuir monolayers. The nanoparticles reported here should be disk-like or semispherical ones.

It can be seen that the ordered structure was formed after daylight illumination. It also can be seen that the nanoparticles grow with time, and the size distribution of the nanoparticles become narrower with time, too, which will be discussed below. In addition, the Ag^+ concentration in the subphase has great effects on the size of the formed nanoparticles. For example, with decreasing the $[Ag^+]$ from 1×10^{-3} to 1×10^{-4} mol L^{-1}, the average diameter of the silver particles increases from 2.97 to 4.94 nm after 31 days.

HRTEM image shown in Figure 1e gives clear lattice fringes. The distance between the adjacent fringes was calculated to be 0.265 nm, which is greater than 0.236 nm, the lattice spacing between the {111} facets of face-centered cubic (fcc) Ag, and less than 0.293 nm, the lattice spacing between the {110} facets of fcc Ag, but close to 0.272 nm, the calculated lattice spacing between the {111} facets of cubic Ag_2O based on the lattice parameter of 0.4726 nm,[31] indicating that nanoparticles may be composed of Ag_2O. According to some literatures, the latticing spacing between the {111} planes of cubic Ag_2O nanoparticles was measured to be 0.265-0.273 nm for Ag_2O nanoparticles by XRD measurements.[25,32,33]

X-ray photoelectron spectroscopy. The composition of the formed structures was checked by XPS, as shown in Figure 2. Two bands appear in the XPS spectrum, which locate at *ca.* 374 and 368 eV, corresponding to $3d_{3/2}$ and $3d_{5/2}$ of silver, respectively. The bands are asymmetric, and can be dissolved into two peaks. For example, the $3d_{5/2}$ band is composed of two peaks, which locate at 367.7 and 368.2 eV with the relative amounts of 93% and 7%, respectively. According to the literatures, the location of the XPS peaks of silver depends on the chemical states of silver element and the size of the nanoparticles.[34,35] The binding energy of the Ag(0) is higher than that of Ag(I), and the binding energy of Ag(0) in smaller clusters is higher than that in bigger nanoparticles. Maybe there are bigger particles in the samples due to the evaporation of the remanent subphase solution on the slides during transfer from the air-water interface. Most possibly, Ag(0) and Ag(I) coexist in the samples. It was reported that small Ag nanoparticles readily react with oxygen, forming Ag_2O and AgO upon exposure to air.[23,36] The binding energies of 368.0-368.3, 367.6-367.8, and 367.3-367.4 eV were reported for pure Ag, Ag_2O, and AgO, respectively.[37,38] So it is reasonable to draw a conclusion that the formed nanoparticles are mainly composed of Ag_2O. This result is coincident to HRTEM observation.

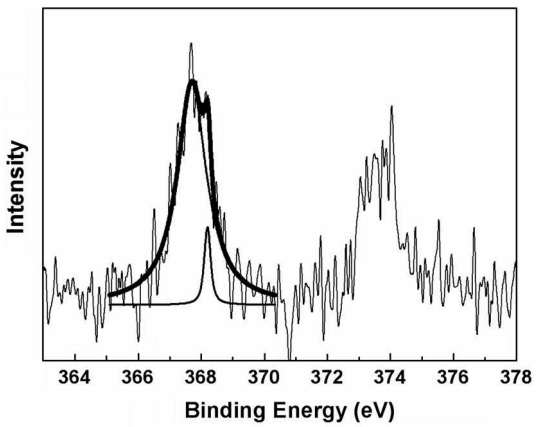

Figure 2. XPS of the transferred film corresponding to Figure 1c.

UV-vis spectroscopy. UV-vis spectrum of the sample is shown in Figure 3. An absorption band and a shoulder appear at *ca.* 265 and 300 nm, respectively. The optical band gap of Ag_2O locates between 2.5-3.1 eV,[32] and the particle plasmon resonance absorption peaks shift from 450 to 420 nm with decreasing the particle size from 87 to 47 nm,[20] showing obvious quantum size effect. With decreasing the particle size further, the absorption peak would be shifted to blue region further. It was reported that the absorption between 250-400 nm was ascribed to silver clusters with different size and oxidation states.[39] According to these literatures, and the HRTEM and XPS results, the absorption band and shoulder shown in Figure 3 should be attributed to smaller silver oxide nanoclusters.

Formation mechanism. We have studied the composite Langmuir monolayers of *n*-HDP/ES/$Eu(phen)_2Cl_3$ in a previous paper.[27] In this paper, the FTIR spectra of pure *n*-HDP and mixed thin films were studied. It was shown that most *n*-HDP molecules form hydrogen bonds in the pure film, while *n*-HDP molecules connected with each other *via*

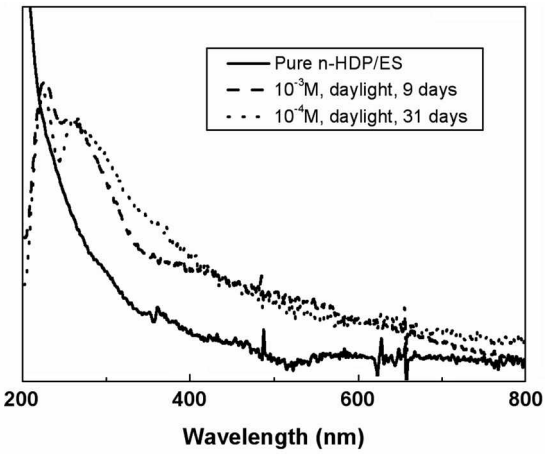

Figure 3. UV-vis spectra of the transferred films of pure n-HDP/ES, the composite films after illumination for 9 days and 31 days on the $AgNO_3$ aqueous solution surfaces with the concentrations of 1×10^{-3} and 1×10^{-4} mol·L^{-1}, respectively.

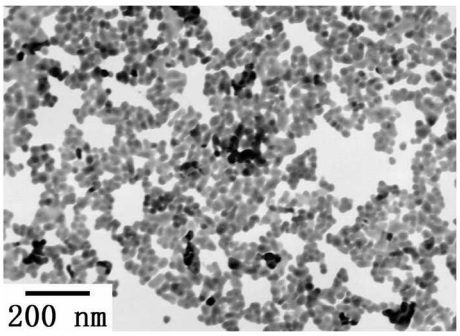

Figure 4. TEM micrograph of silver nanoparticles formed on $AgNO_3$ solution surface by daylight illumination for 9 days without template.

hydrogen bonds and, at the mean while, the complex ions associated to *n*-HDP through electrostatic interactions in the mixed thin films. In addition, parallel aligned nanowires formed in the composite Langmuir monolayers.[27] These results suggest that *n*-HDP molecules may form parallel aligned linear supramolecular structure at the air-water interface through hydrogen banding. We have employed these supramolecular structures as templates to prepare 1D chains of silver oxide nanoparticles.[26]

In the composite monolayers at the air-$AgNO_3$ aqueous solution interface the *n*-HDP molecules formed linear supramolecules through intermolecular hydrogen bonds between the -P=O group and one -OH group, another -OH group can bond Ag^+ ion from the subphase, as shown in Scheme 1.

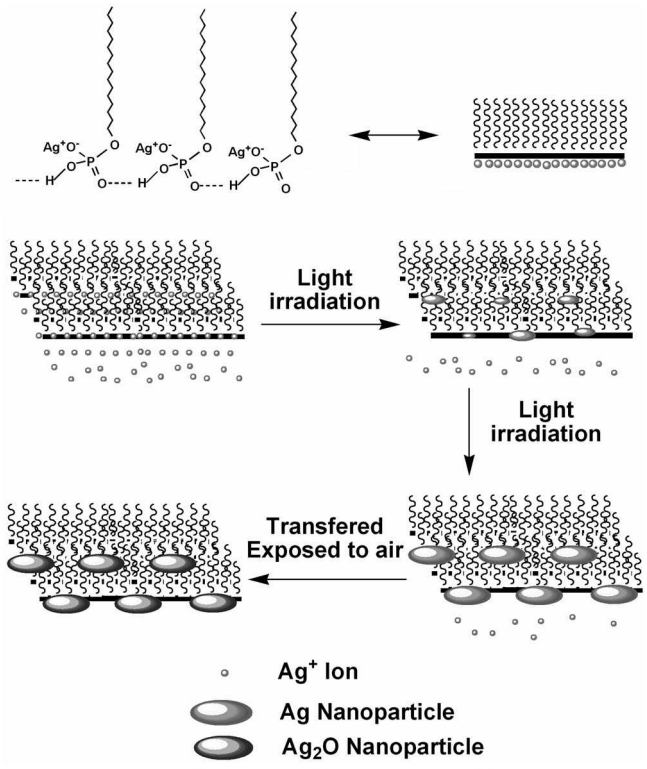

Scheme 1. Schematic representation of the formation of 2D arrays of silver oxide nanoparticles.

When the composite monolayers were illuminated by daylight, Ag^+ ions in the monolayers and at the interfacial phase can be reduced to Ag atoms continuously. The reaction rate is very slow in this case, leading to the formation of very tiny nanoparticles, that is, clusters. During the reaction process, there should be numerous particles with different size formed. These particles have different surface energies, which depend on their size. The bigger particles with lower surface free energy grow slowly, and the smaller ones with higher surface free energy grow rapidly, resulting in similar size at last. It is possible that the parallel aligned linear supramolecules formed by *n*-HDP restrict the region for the nuclei and growth of the silver nanoparticles, so quasi-hexagonal 2D arrays of silver nanoparticles formed. It is clearly seen from Figure 1d that the linear structures play an important role in the formation of the ordered structures.

We have prepared Ag nanoparticles at the air-$AgNO_3$ aqueous solution interface by daylight illuminating without template molecules. Bigger scattered nanoparticles formed as shown in the TEM micrograph in Figure 4, indicating the action of the template molecules.

When the composite monolayers containing 2D arrays of silver nanoparticles were transferred from the air-water interface on solid substrates and exposed to air, oxidation took place, resulting in the formation of 2D arrays of silver oxide nanoparticles. The process is shown in Scheme 1.

Conclusions

2D arrays of silver oxide nanoparticles were prepared firstly by reduction of Ag^+ ions at the air-water interface and then by oxidation of the formed silver nanoparticles in air. The parallel aligned supramolecular template plays an important role in restricting nucleation and growth region for the nanoparticles, leading to the formation of 2D arrays. We wish that the supramolecular template method can be used as a general way to construct various kinds of nanostuctures of metal and semiconductors.

Acknowledgments. The authors thank the financial support of NNSFC (Grant No. 20873078) and Education Ministry of China.

References

1. Evanoff, D. D. Jr.; Chumanov, G. *ChemPhysChem* **2005**, *6*, 1221.
2. Perez, A.; Dupuis, V.; Tuaillon-Combes, J.; Bardotti, L.; Prevel, B.; Bernstein, E.; Melinon, P.; Favre, L.; Hannour, A.; Jamet, M. *Adv. Engineer. Mater.* **2005**, *7*, 475.
3. Maicas, M.; Rodriguez, M.; Lopez, E.; Sanchez, M. C.; Aroca, C.; Sanchez, P. *Computational Mater. Sci.* **2002**, *25*, 525.
4. Nawa, N.; Baba, R.; Nakabayashi, S.; Dushkin, C. *Nano Lett.* **2003**, *3*, 293.
5. Genov, D. A.; Sarychev, A. K.; Shalaev, V. M.; Wei, A. *Nano Lett.* **2004**, *4*, 153.
6. Hossain, M. K.; Shimada, T.; Kitajima, M.; Imura, K.; Okamoto, H. *Langmuir* **2008**, *24*, 9241.
7. Neve-Oz, Y.; Golosovsky, M.; Frenkel, A.; Davidov, D. *Phys. Stat. Sol (a)* **2007**, *204*, 3878.

8. Tang, Z.; Kotov, N. A. *Adv. Mater.* **2005**, *17*, 951.
9. Zhao, S.-Y.; Wang, S.; Kimura, K. *Langmuir* **2004**, *20*, 1977.
10. Liu, Q.; Lu, W.; Ma, A.; Tang, J.; Lin, K.; Fang, J. *J. Am. Chem. Soc.* **2005**, *127*, 5276.
11. Shevchenko, E. V.; Talapin, D. V.; Murray, C. B.; O'Brien, S. *J. Am. Chem. Soc.* **2006**, *128*, 3620.
12. Gattas-Asfura, K. M.; Constantine, C. A.; Lynn, M. J.; Thimann, D. A.; Ji, X.; Leblanc, R. M. *J. Am. Chem. Soc.* **2005**, *127*, 14640.
13. Ji, X.; Wang, C.; Xu, J.; Zheng, J.; Gattas-Asfura, K. M.; Leblanc, R. M. *Langmuir* **2005**, *21*, 5377.
14. Gotoh, A.; Uchida, K.; Kawai, A.; Kamiya, K.; Ikazaki, F.; Sano, S.; Tsuzuki, A. *J. Mater. Sci. Lett.* **2003**, *22*, 1205.
15. Sohn, B.-H.; Choi, J.-M.; Yoo, S. I.; Yun, S.-H.; Zin, W.-C.; Jung, J. C.; Kanehara, M.; Hirata, T.; Teranishi, T. *J. Am. Chem. Soc.* **2003**, *125*, 6368.
16. Gao, F.; Lu, Q.; Komarneni, S. *Chem. Mater.* **2005**, *17*, 856.
17. Swami, A.; Selvakannan, P. R.; Pasricha, R.; Sastry, M. *J. Phys. Chem. B* **2004**, *108*, 19269
18. Khomutov, G. B. *Adv. Colloid Interface Sci.* **2004**, *111*, 79.
19. Lifshitz, Y.; Konovalov, O.; Belman, N.; Berman, A.; Golan, Y. *Adv. Funct. Mater.* **2006**, *16*, 2398.
20. Chiu, Y.; Rambabu, U.; Hsu, M.-H.; Shieh, H.-P. D.; Chen, C.-Y.; Lin, H.-H. *J. Appl. Phys.* **2003**, *94*, 1996.
21. Fukaya, T.; Buchel, D.; Shinbori, S.; Tominaga, J.; Tsai, D. P.; Lin, W. C. *J. Appl. Phys.* **2001**, *89*, 6139.
22. Chuang, C.-M.; Wu, M.-C.; Su, W.-F.; Cheng, K.-C.; Chen, Y.-F. *Appl. Phys. Lett.* **2006**, *89*, 061912.
23. Peyser, L. A.; Vinson, A. E.; Bartko, A. P.; Dickson, R. M. *Science* **2001**, *291*, 103.
24. Zhang, X.-Y.; Pan, X.-Y.; Zhang, Q.-F.; Xu, B.-X.; Jiang, H.-B.; Liu, C.-L.; Gong, Q.-H.; Wu, J.-L. *Acta Phys.-Chem. Sin.* **2003**, *19*, 203.
25. Her, Y.-C.; Lan, Y.-C.; Hsu, W.-C.; Tsai, S.-Y. *Appl. Phys. Lett.* **2003**, *83*, 2136
26. Liu, H.-G.; Xiao, F.; Wang, C.-W.; Xue, Q.; Chen, X.; Lee, Y.-I.; Hao, J.; Jiang, J. *J. Colloid Interface Sci.* **2007**, *314*, 297.
27. Liu, H.-G.; Feng, X.-S.; Xue, Q.-B.; Ji, G.-L.; Wang, S.-Y.; Wang, X.-Y.; Qian, D.-J.; Yang, K.-Z. *Mater. Lett.* **2004**, *58*, 688.
28. He, W.; Jiang, C.; Liu, F.; Tai, Z.; Liang, Y.; Guo, Z.; Zhu, L. *J. Colloid Interface Sci.* **2002**, *246*, 335.
29. Zhao, X. K.; Fendler J. H. *Chem. Mater.* **1991**, *3*, 168.
30. Zhao, X. K.; Fendler J. H. *J. Phys. Chem.* **1991**, *95*, 3716.
31. Li, C.-M.; Robertson, I. M.; Jenkins, M. L.; Hutchison, J. C.; Doole, R. C. *Micron* **2005**, *36*, 9.
32. Gao, X.-Y.; Wang, S.-Y.; Li, J.; Zheng, Y.-X.; Zhang, R.-J.; Zhou, P.; Yang, Y.-M.; Chen, L.-Y. *Thin Solid Films* **2004**, *455-456*, 438.
33. Abe, Y.; Hasegawa, T.; Kawamura, M.; Sasaki, K. *Vacuum* **2004**, *76*, 1.
34. Lopez-Salido, I.; Lim, D. C.; Kim, Y. D. *Surf. Sci.* **2005**, *588*, 6.
35. Luo, K.; St Clair, T. P.; Goodman, D. W. *J. Phys. Chem. B* **2000**, *104*, 3050.
36. Murakoshi, K.; Tanaka, H.; Sawai, Y.; Nakato, Y. *J. Phys. Chem. B* **2002**, *106*, 3401.
37. Weaver, J. F.; Hoflund, G. B. *J. Phys. Chem.* **1994**, *98*, 8519.
38. Tjeng, L. H.; Meinders, M. B. J.; van Elp, J.; Ghijsen, J.; Sawatzky, G. A. *Phys. Rev. B* **1990**, *41*, 3190.
39. Shimizu, K.-i.; Sugino, K.; Kato, K.; Yokota, S.; Okumura, K.; Satsuma, A. *J. Phys. Chem. C* **2007**, *111*, 1683.